Centre for Atmospheric and Oceanic Sciences

INDIAN INSTITUTE OF SCIENCE

BANGALORE 560 012

Validation of SST and Windspeed from TRMM using North Indian Ocean Moored Buoy Observations

Retish Senan, Anitha D. S. and Debasis Sengupta

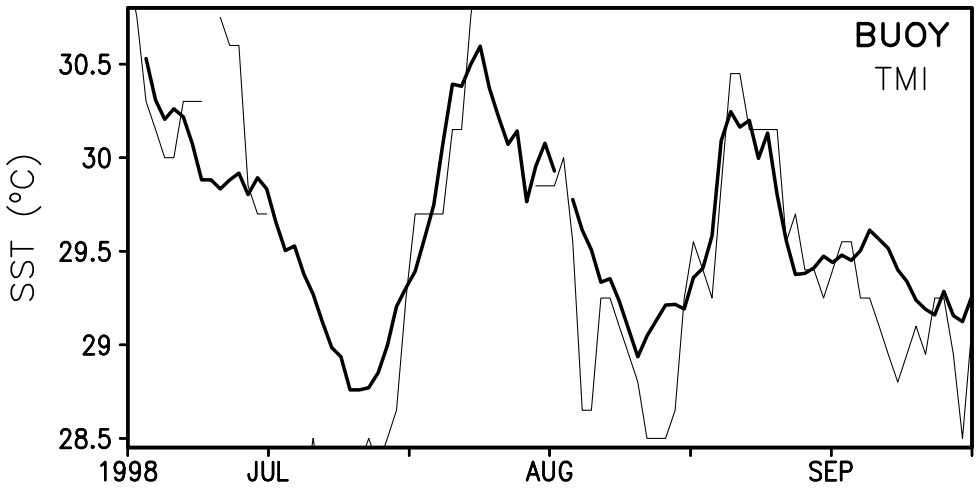

CAOS Report 2001AS1

May 2001

Contents

Validation of SST and Windspeed from TRMM using North Indian Ocean Moored Buoy Observations

Retish Senan, Anitha D. S. and Debasis Sengupta

Center for Atmospheric and Oceanic Sciences, Indian Institute of Science, Bangalore, India.

1 Introduction

Sea Surface Temperature (SST) and wind speed are important surface parameters that determine air-sea interaction in the tropics. Availability of good quality SST and wind speed data with good spatial and temporal resolution is central to study of tropical climate. There has been a paucity of *in situ* data on SST and wind over large regions of the Indian Ocean on time scales of days to weeks. Until a few years back only monthly means of SST and wind were available, such as the Levitus data set and the Coupled Ocean Atmosphere Data Set [*Levitus and Boyer*, 1994; *da Silva et al.*, 1994]. Later, the National Centers for Environmental Prediction (NCEP) Optimally Interpolated (OI) Sea Surface Temperature product [*Reynolds and Smith*, 1994] consisting of weekly and monthly global sea surface temperature fields became available. This product blends ship and buoy SST and satellite derived SST from the NOAA Advanced Very High Resolution Radiometer (AVHRR). One of the greatest limitations in the AVHRR derived SST is the obstruction by clouds. Other sources of error are atmospheric aerosols and water vapour as well as water surface characteristics. In addition, there is lack of *in situ* data over several regions. As a result, the weekly analyses are heavily interpolated and smoothed, especially in the summer monsoon region. Recently, the National Centers for Environmental Prediction/National Center for Atmospheric Research (NCEP/NCAR) Reanalysis Project [*Kalnay et al.*, 1996] has been providing six-hourly fields of zonal and meridional surface wind at a nominal height of 10 metres above the ocean

surface. The NCEP reanalysis uses a global data assimilation system , along with observations from land surface, ship, rawinsonde, pibal, aircraft, satellite and other data to produce global fields of various meteorological parameters [*Kalnay et al.*, 1996]. The reanalysis also uses delayed observations, thereby increasing the reliability of the wind and other products. Over the north Indian Ocean the NCEP reanalysis wind captures variability on all time scales longer than a few days [*Sengupta et al.*, 1999]. Very recently, a new satellite product has become available that provides simultaneous measurements of SST and wind with high spatial resolution.

1.1 Tropical Rainfall Measuring Mission

The Tropical Rainfall Measuring Mission (TRMM) is a joint mission of the U. S. National Aeronautics and Space Administration (NASA) and the National Space Development Agency (NASDA) of Japan designed to monitor and study tropical rainfall and the associated release of energy. The TRMM satellite carries five instruments: The first spaceborne Precipitation Radar, the TRMM Microwave Imager (TMI), a Visible and Infrared Scanner, a Cloud and Earth Radiant Energy System, and a Lightning Imaging Sensor. The TRMM Microwave Imager is similar to SSM/I and contains lower frequency channels required for sea surface temperature retrievals.

The measurement of SST and wind speed by microwave radiometers is based on the principle that the emissivity of the ocean is a function of SST, salinity and winds. Passive microwave radiometers onboard earth observing satellites measure emission from the ocean-atmopshere system in the microwave frequency bands. This radiation follows the Rayleigh Jeans limit of Planck's radiation law, and is expressed in terms of the Brightness Temperature. Retrieval of ocean-atmospheric parameters parameters using brightness temperature requires measurement to be made at multiple frequencies and polarisations supported by sophisticated modelling of radiative transfer.

The measurement of SST through clouds by satellite microwave radiometers has been an elusive goal for many years. The early radiometers in the 1980's (i.e., SMMR) were poorly calibrated, and the later radiometers (i.e., SSM/I) lacked the low frequency channels needed by the retrieval algorithm. The TMI radiometer has a 10.7 GHz channel. The important

feature of microwave retrievals is that SST can be measured through clouds, which are nearly transparent at 10.7 GHz. This is a distinct advantage over the traditional infrared SST observations that require a cloud-free field of view. Ocean areas with persistent cloud coverage can now be viewed on a daily basis. Furthermore, microwave retrievals are not affected by aerosols and are insensitive to atmospheric water vapor. The TMI also measures wind speeds derived using two different radiometer channels. Microwave observations are an ideal way to observe the interaction between SST and wind because both the parameters can be simultaneously retrieved.

The TMI SST and wind has provided insights into a number of areas including the interaction of Atlantic hurricanes and SST [*Wentz et al.*, 2000]. In the equatorial eastern pacific , signatures of tropical instability waves (TWI) associated with the equatorial ocean current system are prominently seen in the TMI SST and wind fields [*Chelton et al.*, 2000]. TMI is capable of reproducing the SST and wind variability over the warm tropical ocean on all time scales from a few days to interannual.

However, TMI SST and wind have not been validated over the Indian Ocean. In this report we validate the TMI SST and wind speed over the north Indian Ocean by comparing it with buoy-measured SST and wind speed. We also compare the large scale features of the TMI data with climatalogical SST and wind, in addition to aspects of the annual cycle and interannual variability.

2 DATA

The TMI SST and wind speed fields are on a 0.25 by 0.25°grid. Except over a few regions of persistent rain, TMI provides complete coverage in three days. Therefore we use the three-day running mean data provided by *Remote Sensing Systems, Santa Rosa, CA* from their site *ftp://ftp.ssmi.com*. Apart from TMI data, we use 3m SST and 3.2m wind from a network of met-ocean buoys (Figure 1; Table 1) installed by the Department of Ocean Development (DOD), New Delhi under the National Data Buoy Programme (NDBP) in September 1997; weekly Reynolds SST, daily averaged winds at 10m height from the NCEP/NCAR reanalysis, climatological SST from the Levitus atlas [*Levitus and Boyer*, 1994] and climatological wind speed from the Coupled Ocean Atmosphere Data Set (COADS)[*da Silva et al.*, 1994].

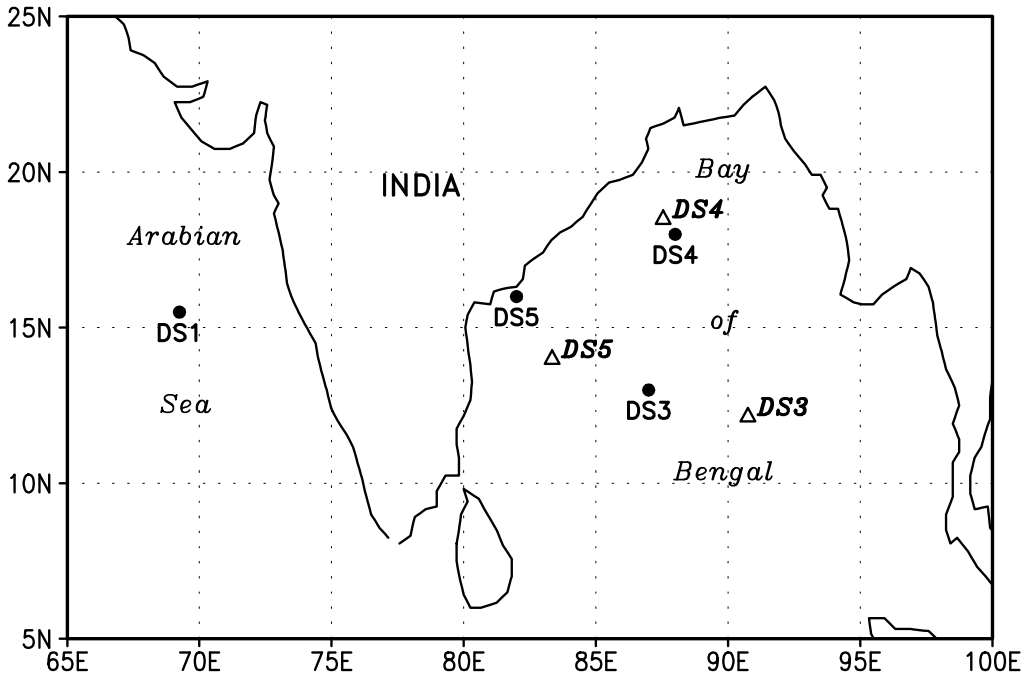

Figure 1: The location of moored met-ocean buoys in the north Indian Ocean. Closed circles indicate location during 1997-1999, while triangles indicate the location in 2000. The location of DS1 is unchanged from 1997-2000.

3 METHOD

We use three-day running means of SST and wind speed from the buoy data in all our comparisons, since the TMI SST and wind speed are effectively three-day running means. Periods of apparent spurious values from the buoys are eliminated from the comparison.

	1998	1999	2000
DS1	15.5°N 69.25°E	15.5°N 69.25°E	15.5°N 69.25°E
DS3	13°N 87°E	13°N 87°E	12.15°N 90.75°E
DS4	19°N 89°E (Jan-Mar) 18°N 88°E (Jun-Dec)	18°N 88°E	18.5°N 87.55°E
DS5	16°N 82°E		14°N 83.35°E

Table 1: DOD met-ocean buoy locations.

The buoy time series are compared with TMI by taking the grid point nearest to the buoy locations (Table 1). For comparisons of wind speed, the buoy wind speed is stepped up to 10m height, by assuming a logarithmic wind profile [*Rao and Premkumar*, 1998], according to

$$U_{10} = U_z \left(\frac{10}{z} \right)^{1/7}$$

where U_z is the wind speed at height z, and U_{10} is the wind speed at 10m. The buoy wind speed is reported at 3.2m. Thus using the above relation, the equivalent wind speed at 10m can be obtained by multiplying the buoy wind speed by 1.177. The statistics used in the comparison are TMI and buoy standard deviation, and correlation coefficients, mean difference and root-mean-square difference between TMI and buoy measurements.

4 Comparsion of Seasonal Means

4.1 SST

The seasonal mean SST from TMI, Reynolds and Levitus climatology are compared. TMI and Reynolds SST are averages over 1998-2000, while the Levitus climatology is based on almost one hundred years of ship reports. The winter mean (December-February; DJF) SST from TMI (Figure 2) shows large scale features similar to Reynolds and Levitus climatology. The warmest waters are to the south of the equator in the three products. The contours are zonally oriented in the western north equatorial Pacific. The patch of warm water ($> 30°$C) north and east of Madagascar in TMI is absent in Reynolds and Levitus. DJF northeast Indian Ocean SST is shown in Figure 4a. The TMI product might have unreliable SST at the grid point nearest to coasts and islands.

Prominent in the summer (June-September; JJAS) mean SST field is warm temperatures in the western equatorial Pacific in TMI when compared to Reynolds and Levitus (Figure 3). The warmest water in this region is a degree higher in TMI than in Levitus. The SST is cool to the south and east of Sri Lanka due to upwelling and advection (Figure 4b). Levitus is cooler than the other two products in both seasons, perhaps because it is the bulk sea surface temperature. The warm water in the west and north Bay of Bengal has a larger extent in Reynolds compared to TMI.

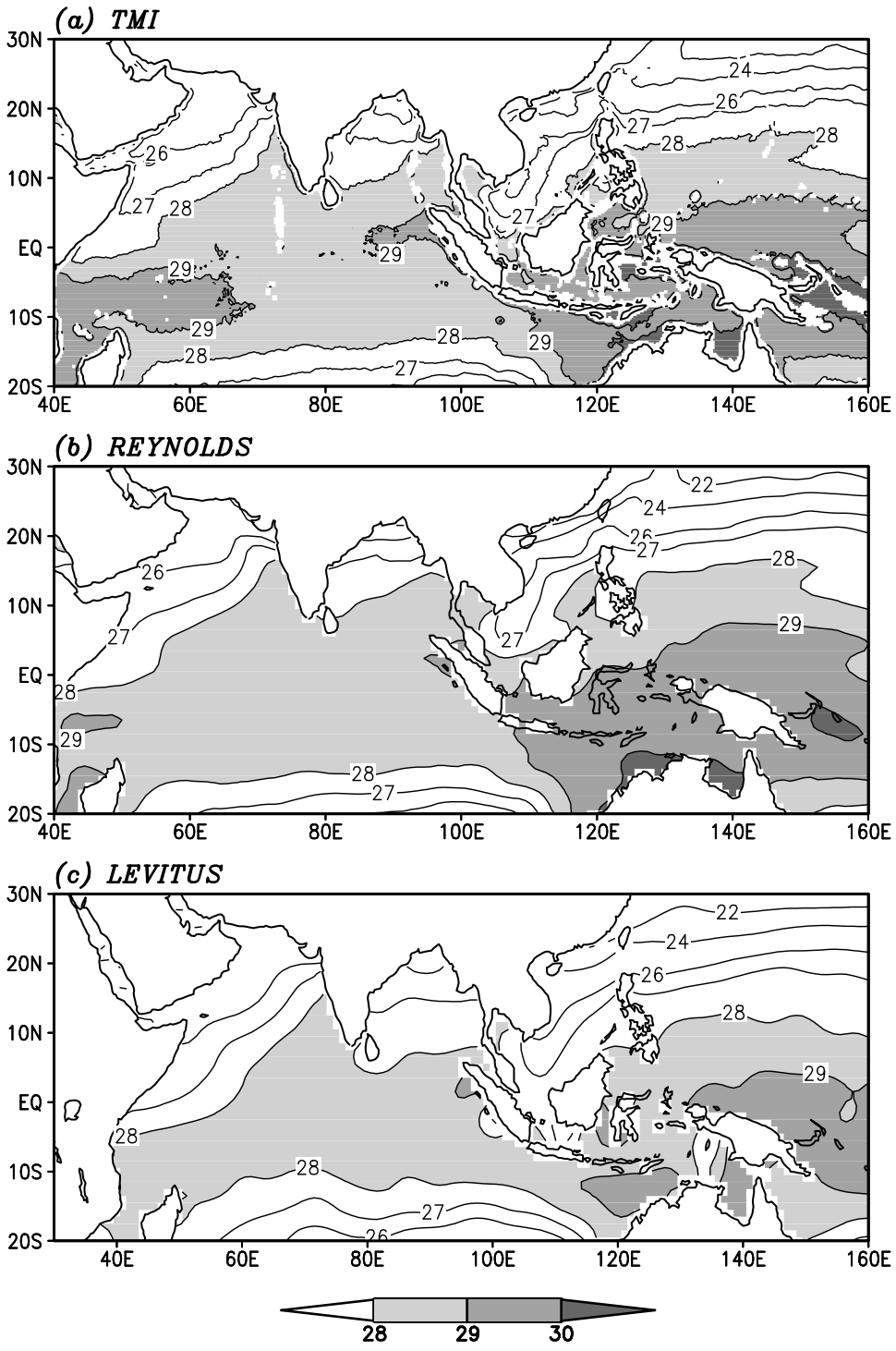

Figure 2: Winter mean (December-February) Sea Surface Temperature (°C) from (a) TMI (b) Reynolds and (c) Levitus

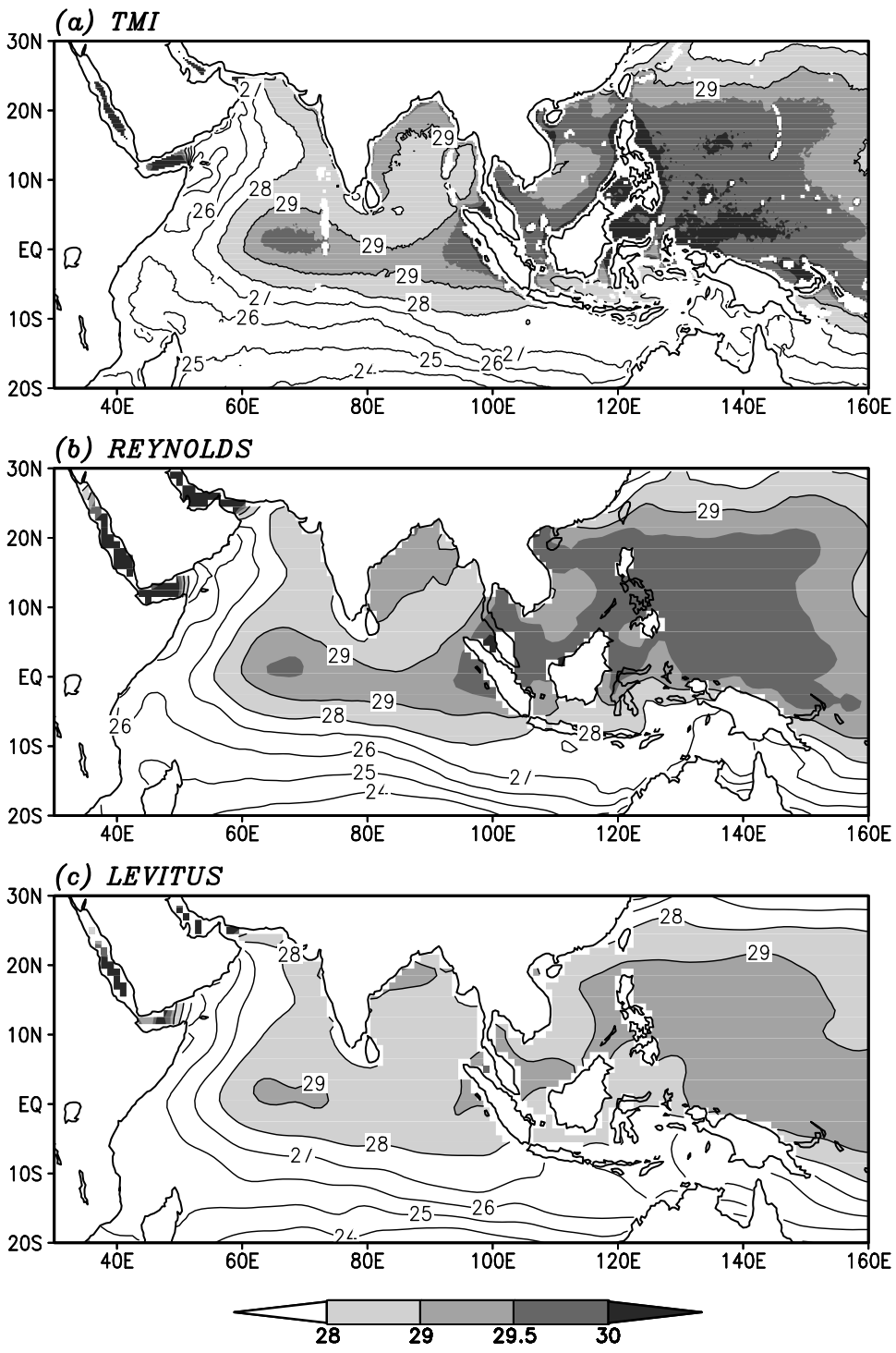

Figure 3: Summer mean (June-September) Sea Surface Temperature (°C) from (a) TMI (b) Reynolds and (c) Levitus

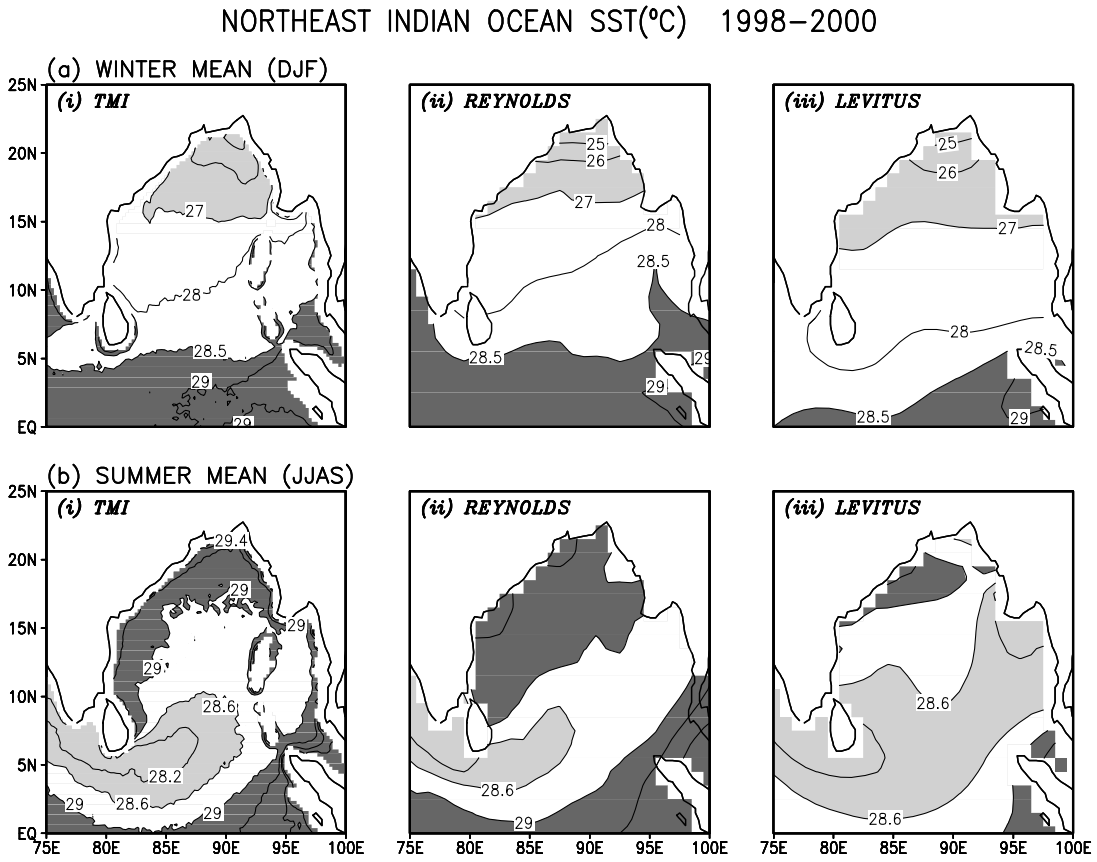

Figure 4: (a) Winter mean (December-February) and (b) Summer mean (June-September) Sea Surface Temperature (°C) in the North Indian Ocean from (i) TMI (ii) Reynolds and (ii) Levitus

Figure 5 depicts a three-year composite of the evolution of TMI SST in the northeast Indian Ocean during the summer monsoon. In May the entire region is warm with SST exceeding 29°C. With the onset of strong monsoon winds, cooling extends eastward from the southern tip of India and Sri Lanka in June; the southern Bay of Bengal cools more than the central and northern Bay. By August, the cool waters extend to almost the entire Bay, before retreating southward in October.

4.2 Windspeed

The seasonal mean wind speed from TMI are compared with those from the NCEP/NCAR reanalysis and the COADS climatology. TMI and NCEP wind speed are averages over 1998-2000, while the COADS climatology is based on many decades of data. The winter mean (DJF) wind speed from NCEP are systematically weaker than TMI or COADS over most

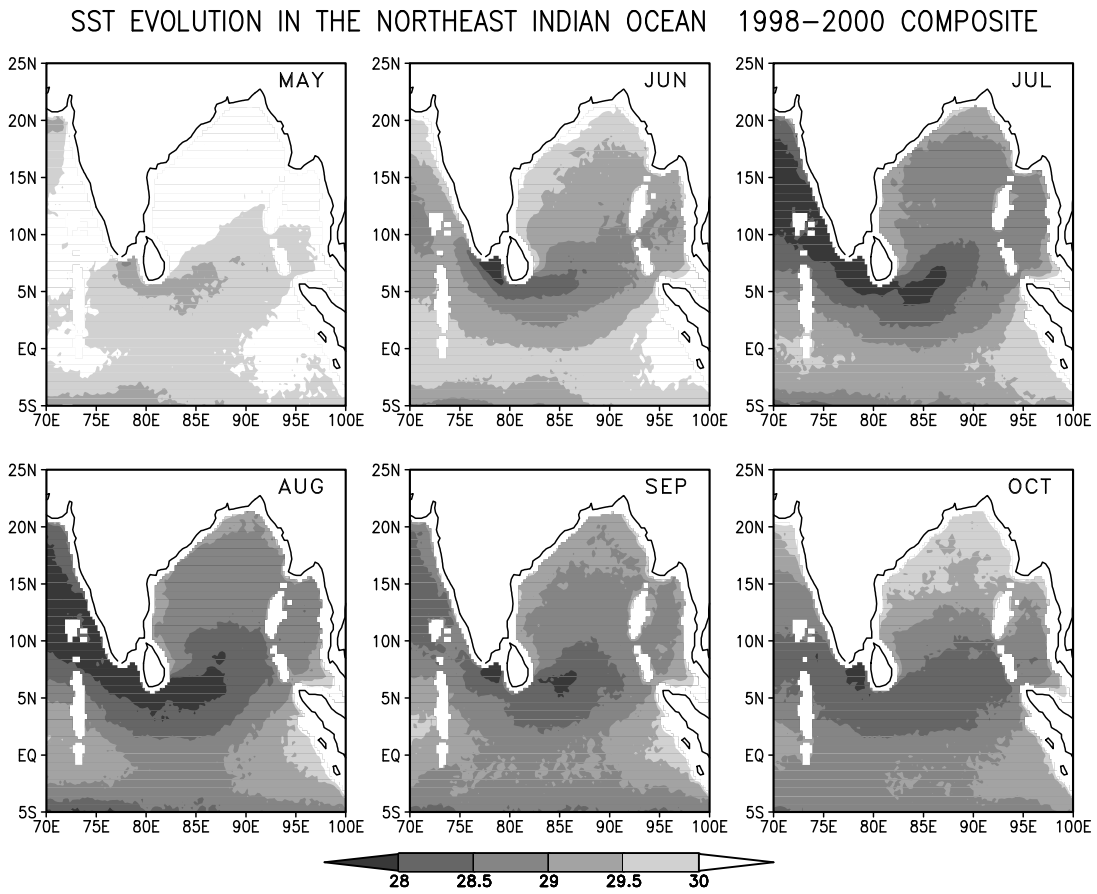

Figure 5: Mean evolution of TMI SST over the northeast Indian Ocean during May to September

parts of the Indian Ocean and West Pacific (Figure 6). The region of high wind speed (> 9 ms^{-1}) in the South China Sea in TMI is almost absent in NCEP, while its is slighly stronger in COADS.

Like the winter mean, the summer mean wind speed from NCEP is also systematically weaker than TMI or COADS over most of the Indian Ocean and West Pacific (Figure 7). The NCEP wind speed in the equatorial region and the entire west Pacific is particularly weak, perhaps due to problems with the data assimilation system. The patch of strong winds (> 10 ms^{-1}) in the southern Indian Ocean in TMI is almost absent in COADS and NCEP. Summer monsoon winds of > 8 ms^{-1} cover almost the entire Arabian Sea and Bay of Bengal in the TMI product; the spatial extent of high winds is slightly smaller in COADS.

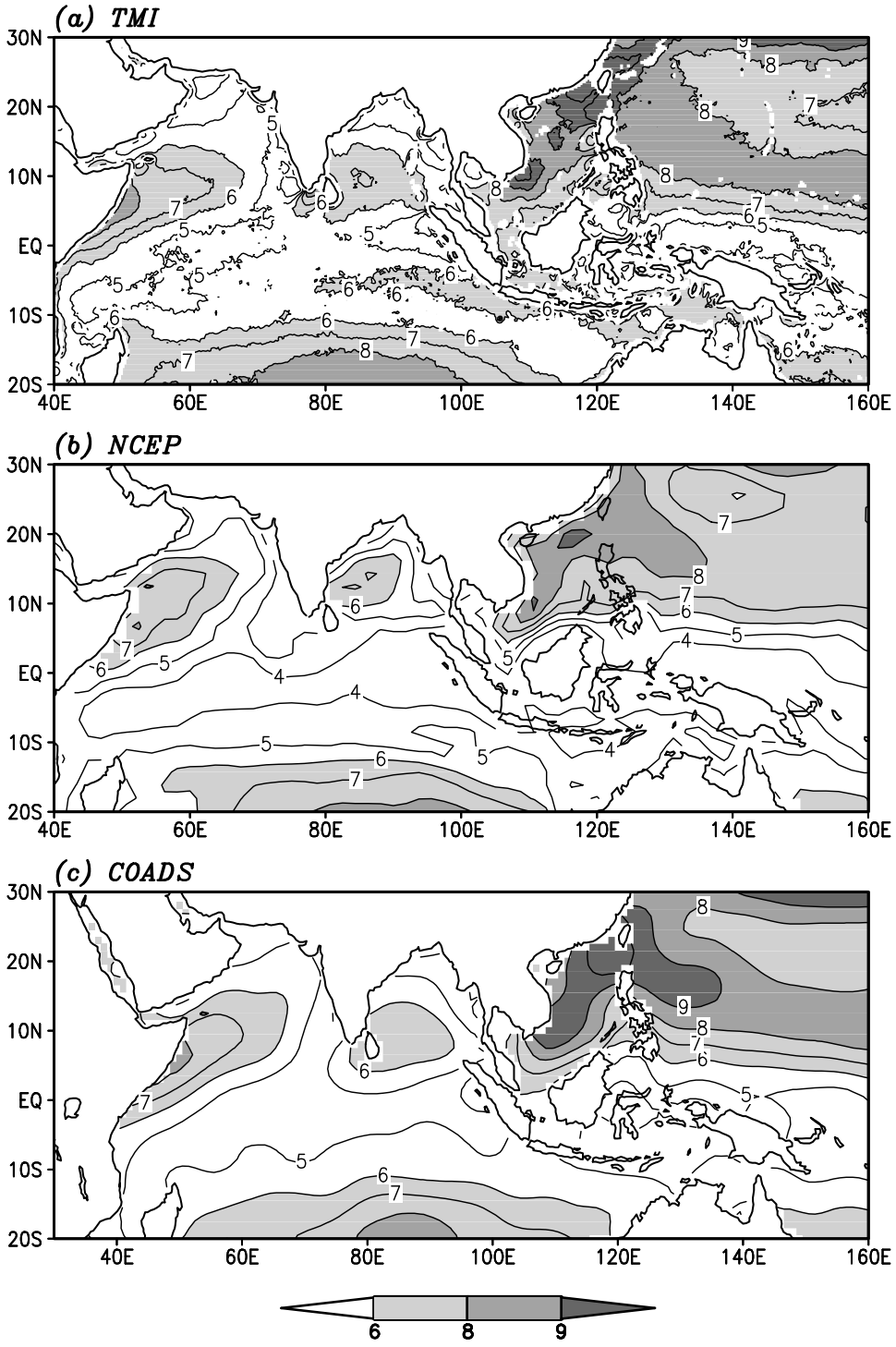

Figure 6: Winter mean (December-February) Windspeed (ms^{-1}) from (a) TMI (b) NCEP and (c) COADS

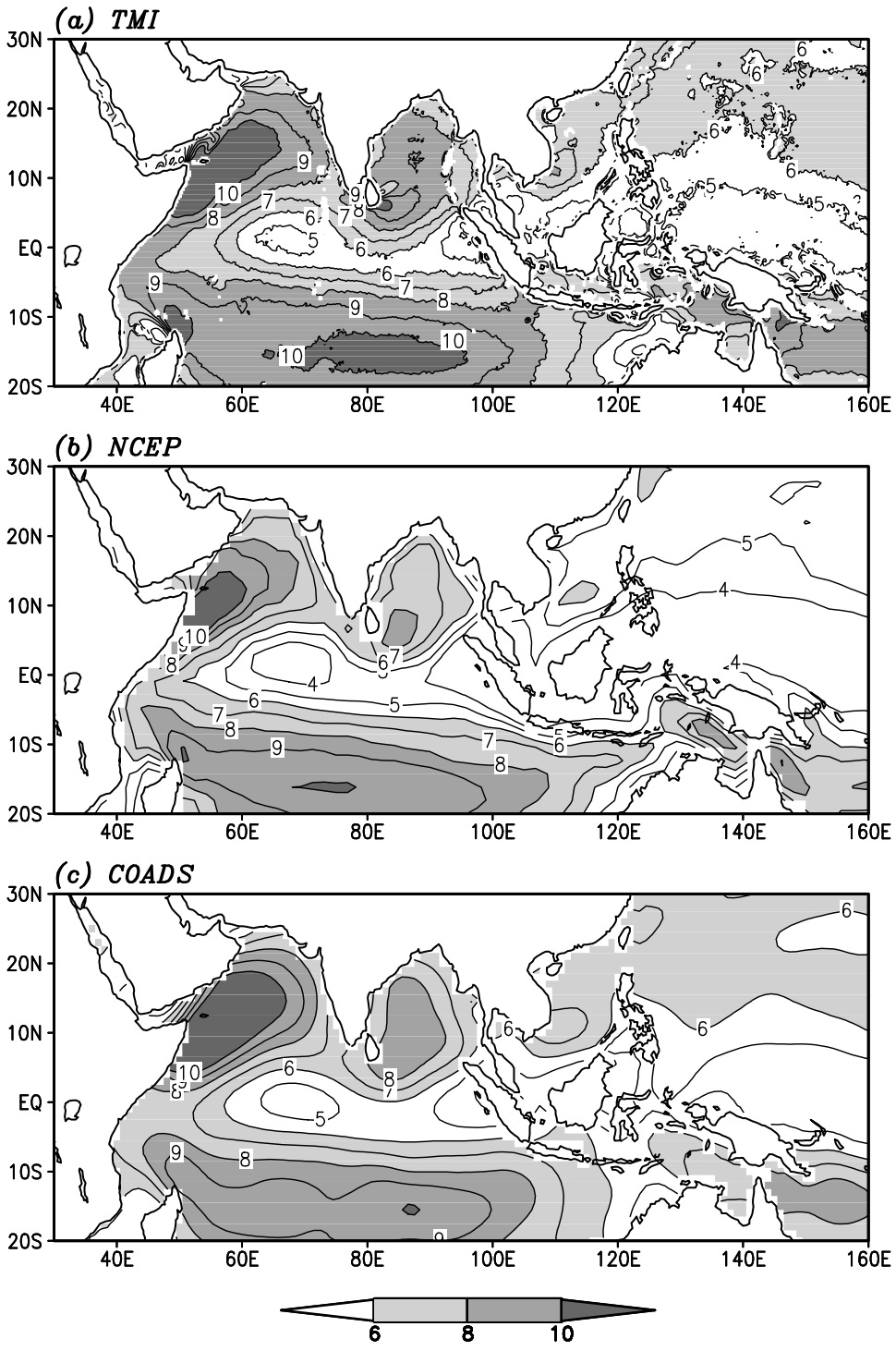

Figure 7: Summer mean (June-September) Windspeed (ms^{-1}) from (a) TMI (b) NCEP and (c) COADS

5 Comparsion of Buoy and TMI SST

Three day running mean SST from DOD met-ocean buoys are compared with TMI SST at different locations in the Arabian Sea and Bay of Bengal for the period 1998-2000. Also included in the comparison is the well known NCEP, or Reynolds, weekly SST product.

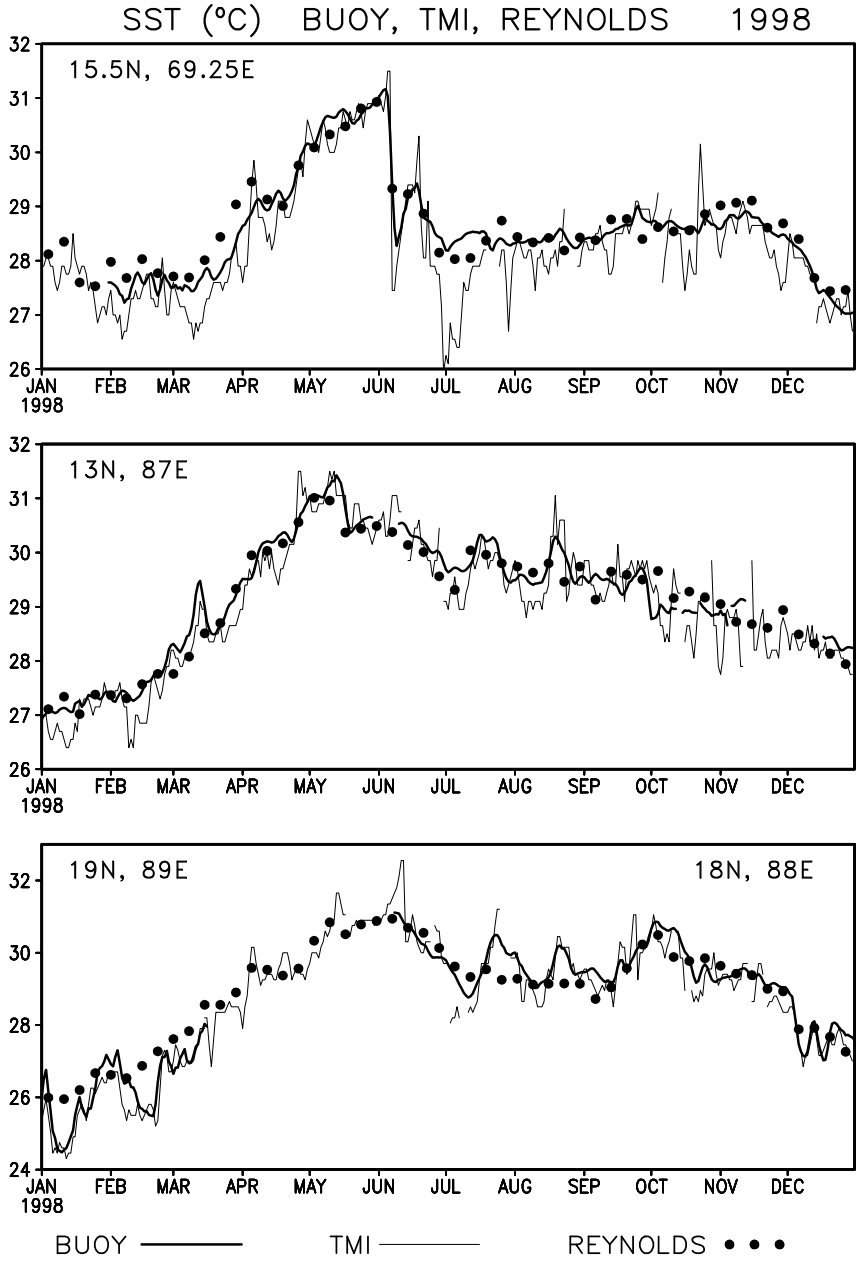

Figure 8: Sea Surface Temperature (°C) in 1998 from buoy (bold line), TMI (thin line) and Reynolds (dots) at 15.5°N, 69.25°E (top), 13°N, 87°E (middle) and 19°N, 89°E (bottom).

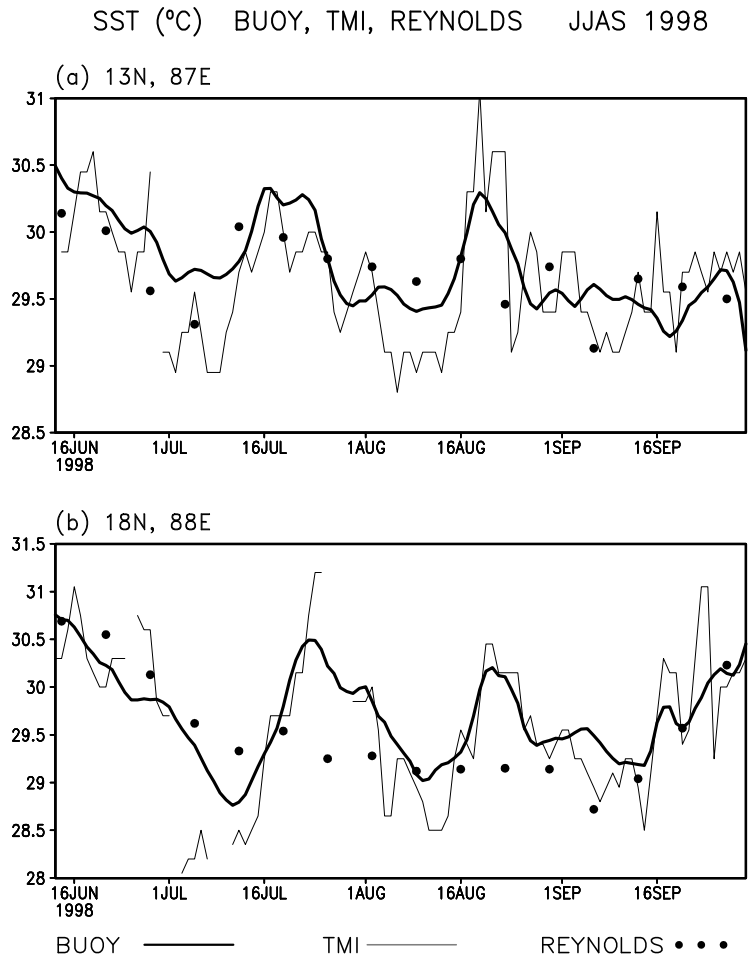

Figure 9: Sea Surface Temperature (°C) from buoy (bold line), TMI (thin line) and Reynolds (dots) at 13°N, 87°E (top) and 18°N, 88°E (bottom) during June to September 1998.

Shown in Figure 8 is a comparison of SST from TMI, buoy and Reynolds at three buoy locations for the year 1998. At all the three locations, the TMI SST captures the annual cycle, and the intraseasonal variability on time scales longer than a few days. The correlation coefficient between TMI and buoy SST at the three buoy locations are 0.907, 0.958 and 0.970. The respective root-mean-square differences are 0.561, 0.399 and 0.472°C (Table 2). This is consistent with the root-mean-square values obtained from a validation with a much larger data set in the Pacific and Atlantic, where Wentz et al. (2000) obtained a mean value of 0.6°C. The standard deviation of the buoy and TMI SST, computed for periods when both data are available, are comparable at most buoy locations (Table 3). The mean difference between TMI and buoy SST averaged over all the buoy locations is about -0.2°C. The 30

day oscillation of SST in the Bay of Bengal during the summer monsoon of 1998 is captured by the TMI SST (Figure 9), whereas it is absent in the Reynolds SST. TMI SST also shows the cooling of the ocean associated with cyclones [*Wentz et al.*, 2000], e.g. the abrupt drop in SST by more than three degrees at 15.5°N, 69.25°E in the Arabian Sea, associated with the passage of a cyclone in early June 1998. Although Reynolds SST is not able to capture much of the intraseasonal variability in summer, it does follow seasonal changes very closely i.e., it represents the seasonal cycle well in all three years.

	1998		1999		2000	
	Corr.	*rms*	*Corr.*	*rms*	*Corr.*	*rms*
DS1	0.907	0.561	0.904	0.434	-	-
DS3	0.958	0.399	0.713	0.529	0.585	0.606
DS4	0.970	0.472	-	-	0.921	0.499
DS5	-	-	-	-	0.916	0.463

Table 2: Correlation coefficient and root-mean-square difference (°C) between TMI and Buoy SST at different buoy locations.

	1998		1999		2000	
	Buoy	*TMI*	*Buoy*	*TMI*	*Buoy*	*TMI*
DS1	0.920	1.122	0.928	0.956	-	-
DS3	1.123	1.237	0.399	0.662	0.275	0.589
DS4	1.644	1.794	-	-	1.118	1.245
DS5	-	-	-	-	0.994	1.099

Table 3: Standard deviation of TMI and Buoy SST (°C) at different buoy locations.

The apparent high frequency variability of TMI SST that is absent in the buoy SST is a reflection of the fact that the TMI SST is the skin temperature, whereas the buoy measures the bulk SST. Bulk SST is representative of the temperature of the upper few metres of the ocean. Skin SST is the temperature of the surface skin of the ocean, which is less than a mm thick [*Grassl*, 1976]. It is found that relatively small changes in wind speed, short wave solar flux, long wave flux and humidity can increase skin temperature variability. Over

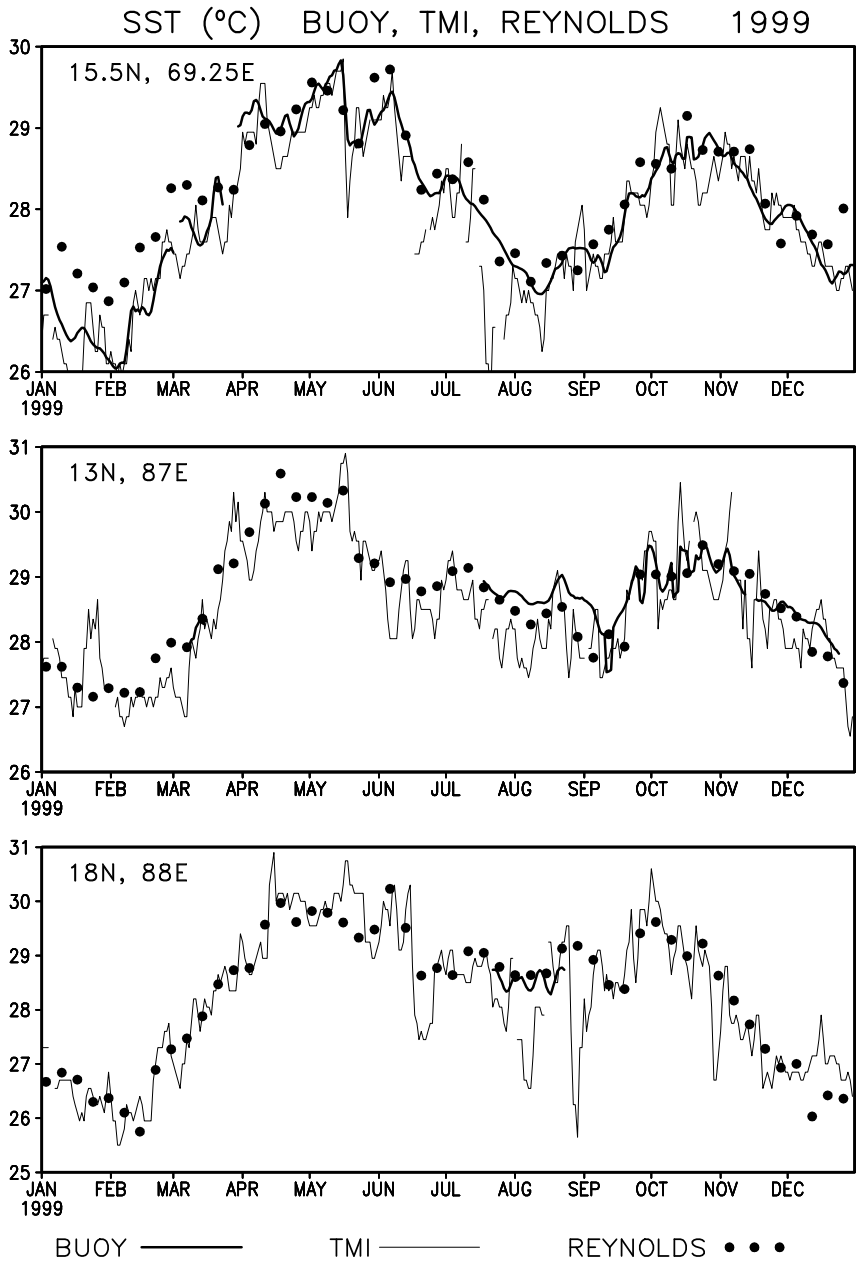

Figure 10: Sea Surface Temperature (°C) in 1999 from buoy (bold line), TMI (thin line) and Reynolds (dots) at 15.5°N, 69.25°E (top), 13°N, 87°E (middle) and 18°N, 88°E (bottom).

equatorial regions, with lower wind speeds, high humidity and air temperature close to ocean temperature, the skin effect is smaller. Under calm conditions with strong solar insolation an unmixed layer can form right near the surface which is up to 1.0°C warmer than the bulk temperature below [*Schlussel et al.*, 1990]. Observations in the tropical Pacific suggests that wind speed affects bulk-skin temperature difference ($\triangle$T) through the net heat flux and

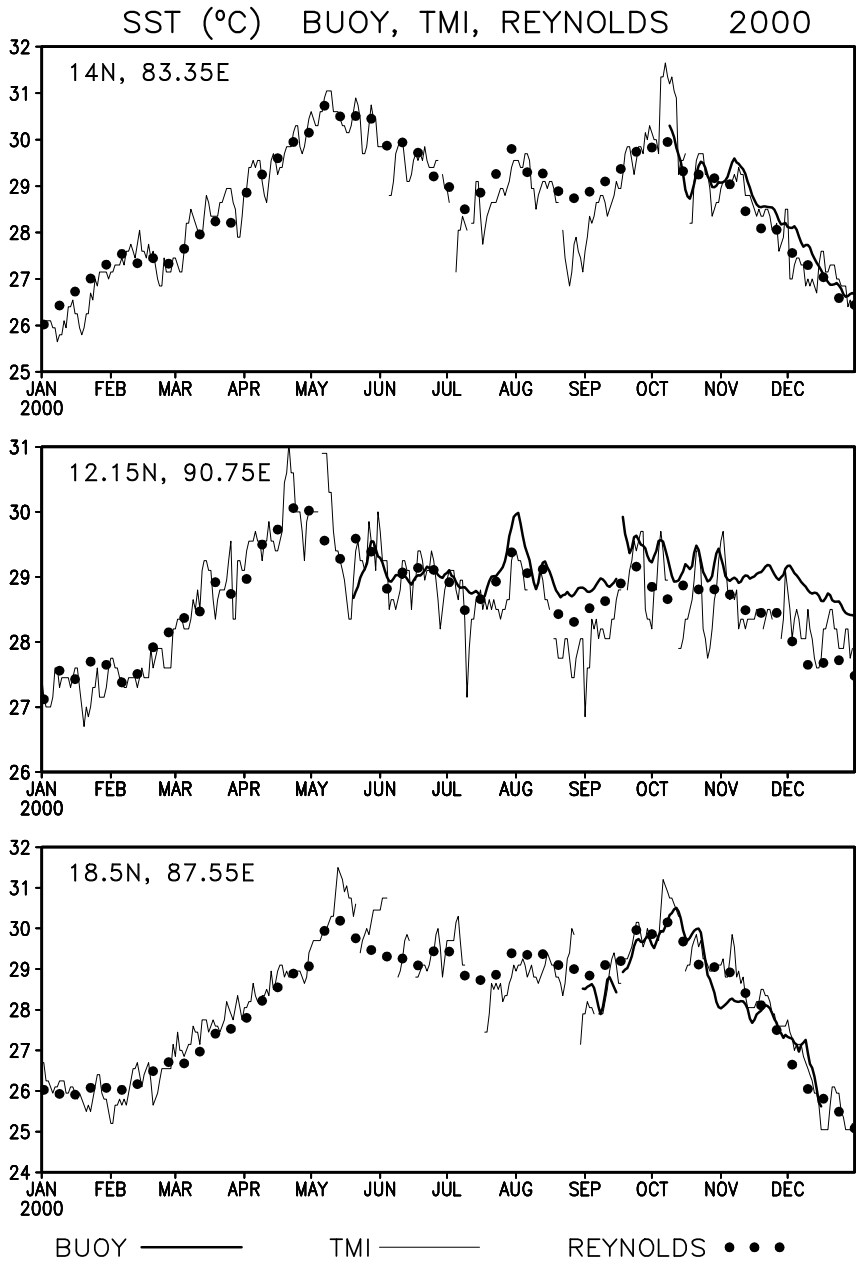

Figure 11: Sea Surface Temperature (°C) in 2000 from buoy (bold line), TMI (thin line) and Reynolds (dots) at 14°N, 83.35°E (top), 12.15°N, 90.75°E (middle) and 18.5°N, 87.55°E (bottom).

turbulent mixing. Increased winds typically increase the magnitude of the turbulent (i.e. latent and sensible) heat loss from the ocean, thus cooling the ocean surface and increasing the size of $\triangle$T. At the same time, increased winds cause enhanced mixing, which tends to decrease $\triangle$T [*Wick et al.*, 1996]. It is further suggested that if a decrease in wind speed leads only to a small change in the heat flux, $\triangle$T will likely increase, while if a decrease in

wind speed leads to a significant drop in heat loss such as when latent heat flux dominates, $\triangle$T is likely to decrease.

Figure 10 and 11 show the comparison of TMI with buoy SST for the years 1999 and 2000. In spite of the non-availability of buoy data over large periods at certain locations, we show the annual cycle of TMI SST to illustrate the fact that it shows large high frequency variability which is generally smaller in Reynolds SST. We wish to point out a possible warm bias in the buoy SST at DS3 (12.15°N, 90.75°E) after mid-september 2000 based on the comparison (Figure 11) with the TMI and Reynolds data. There are occasions when TMI SST shows values that are much cooler or warmer than buoy SST in the neighbourhood of missing data due to rain (e.g. see Figure 9, around 2 July and 25 July). We do not know whether these data are reliable, because of the possibility that there is a problem with the retrieval algorithm in the presence of rainfall.

6 Comparison of Buoy and TMI Wind

Three day running mean of wind speed from DOD met-ocean buoys are compared with TMI wind speed at different locations in the Arabian Sea and Bay of Bengal for the period 1998-2000.

Shown in Figure 12 is the comparison of TMI and buoy wind speed at three buoy locations. The TMI wind speed faithfully captures all variability on time scales larger than a few days. The sudden increase and fall in wind speed associated with the June 1998 cyclone is well captured by TMI. The correlation coefficient between TMI and buoy wind speed at the three buoy locations are 0.887, 0.875 and 0.884 (Table 4). The corresponding root-mean-square differences are 1.421, 1.139 and 1.224 ms^{-1} respectively. The standard deviation of the buoy and TMI wind speed are computed for periods when both data are available; they are comparable at most buoy locations (Table 5). The mean difference between TMI and buoy wind speed averaged over all the buoy locations is less than -0.1 ms^{-1}.

Figure 13 and 14 shows the comparsion of wind speed for 1999 and 2000 at different buoy locations.

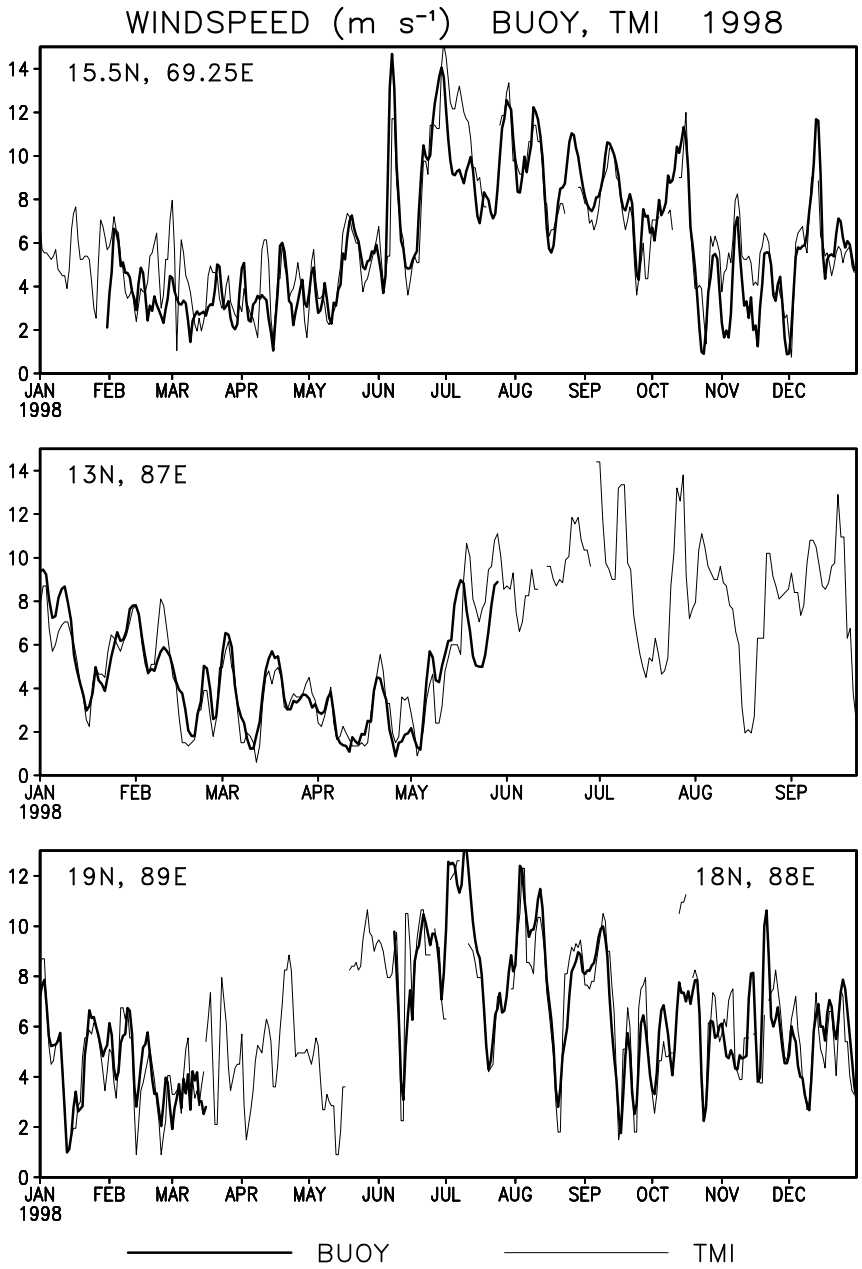

Figure 12: Wind speed (ms^{-1}) in 1998 from buoy (bold line) and TMI (thin line) at 15.5°N, 69.25°E (top), 13°N, 87°E (middle) and 19°N, 89°E (bottom).

7 Interannual variability

7.1 SST

TMI SST exhibits large year-to-year differences at several regions in the north Indian ocean and western equatorial Pacific. Shown in Figure 15 is the summer mean SST difference

	1998		1999		2000	
	Corr.	*rms*	*Corr.*	*rms*	*Corr.*	*rms*
DS1	0.887	1.421	0.975	1.157	0.739	1.117
DS3	0.875	1.139	0.926	1.112	0.895	1.230
DS4	0.884	1.224	0.966	1.725	0.837	1.625

Table 4: Correlation coefficient and root-mean-square difference (ms^{-1}) between TMI and Buoy wind speed at different buoy locations.

	1998		1999		2000	
	Buoy	*TMI*	*Buoy*	*TMI*	*Buoy*	*TMI*
DS1	3.031	3.083	2.878	2.625	1.624	1.401
DS3	2.179	2.390	2.710	2.777	2.601	2.431
DS4	2.570	2.600	2.126	3.004	2.822	2.632

Table 5: Standard deviation of TMI and Buoy wind speed (ms^{-1}) at different buoy locations.

between 1998 and 1999 over the Asian monsoon region, from TMI and Reynolds. The two products agree remarkably well. Almost the entire IMR region is warmer in 1998. The regions of warmest waters are the Bay of Bengal, South China Sea, western Arabian Sea and the Indonesian throughflow region.

The bottom panels in Figure 15 show the TMI SST time series in 1998 and 1999, averaged over $5 \times 5°$boxes in the Bay of Bengal and southern South China Sea. At both these locations, the SST in 1999 fell in the month of May with the onset of strong summer monsoon winds (Figure 13). This fall was much smaller in 1998, and the SST tended to oscillate around a higher value throughout the summer monsoon.

Figure 16 shows the SST difference between 1998 and 2000. Again, 1998 tends to be warmer than 2000, and the regions of warmest differences are similar. Thus, 1998 was an exceptional year with large anomalous warming in the Asian monsoon region. Note also that the intraseasonal SST variability in the southern South China Sea is very small in 1998 compared to 1999 or 2000. Just how anomalous the warm Indian Ocean 1998 SST was can

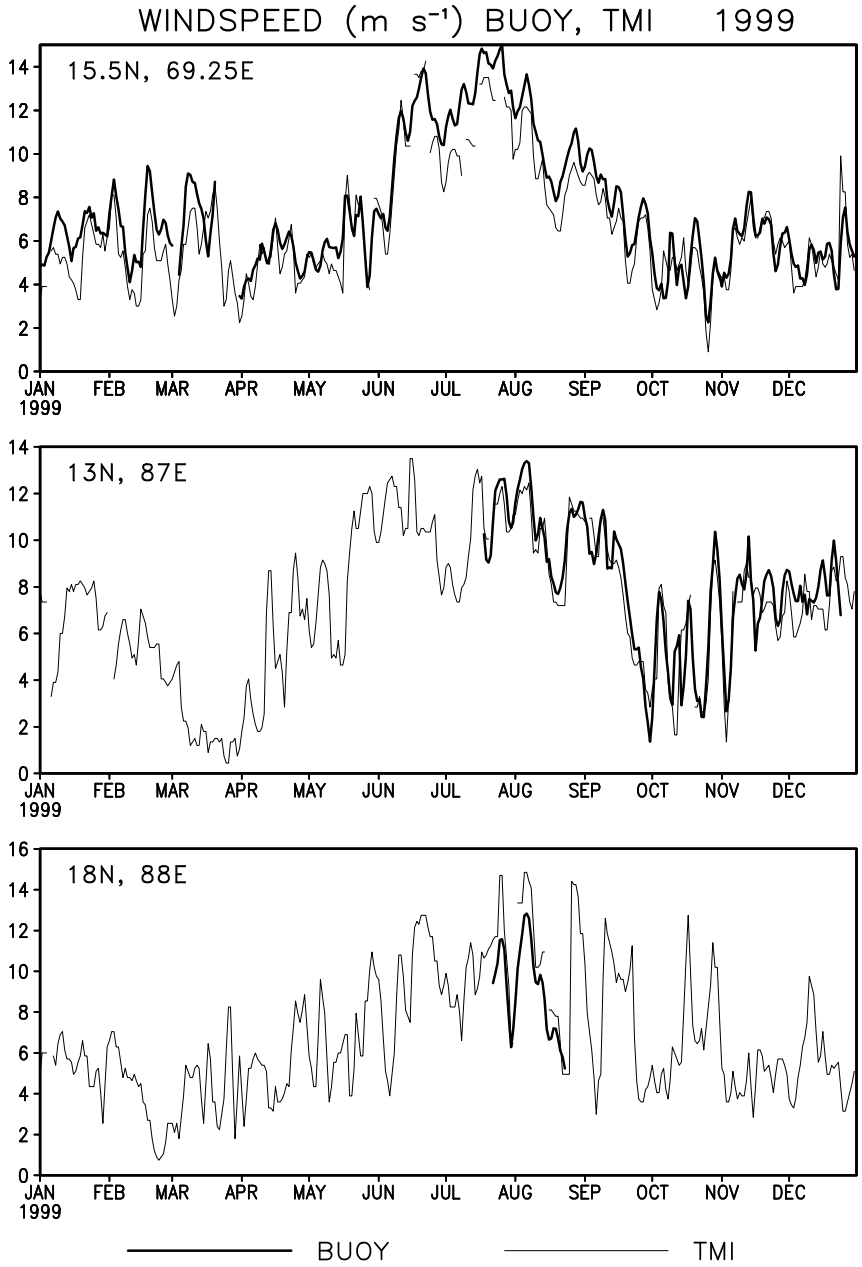

Figure 13: Wind speed (ms^{-1}) in 1999 from buoy (bold line) and TMI (thin line) at 15.5°N, 69.25°E (top), 13°N, 87°E (middle) and 18°N, 88°E (bottom).

be seen from the fact that the entire region (40°E-120°E, 5°N-25°N) was warmer by upto 1.5°C from mid-April to mid-September 1998 compared to 1999 or 2000 (Figure 19).

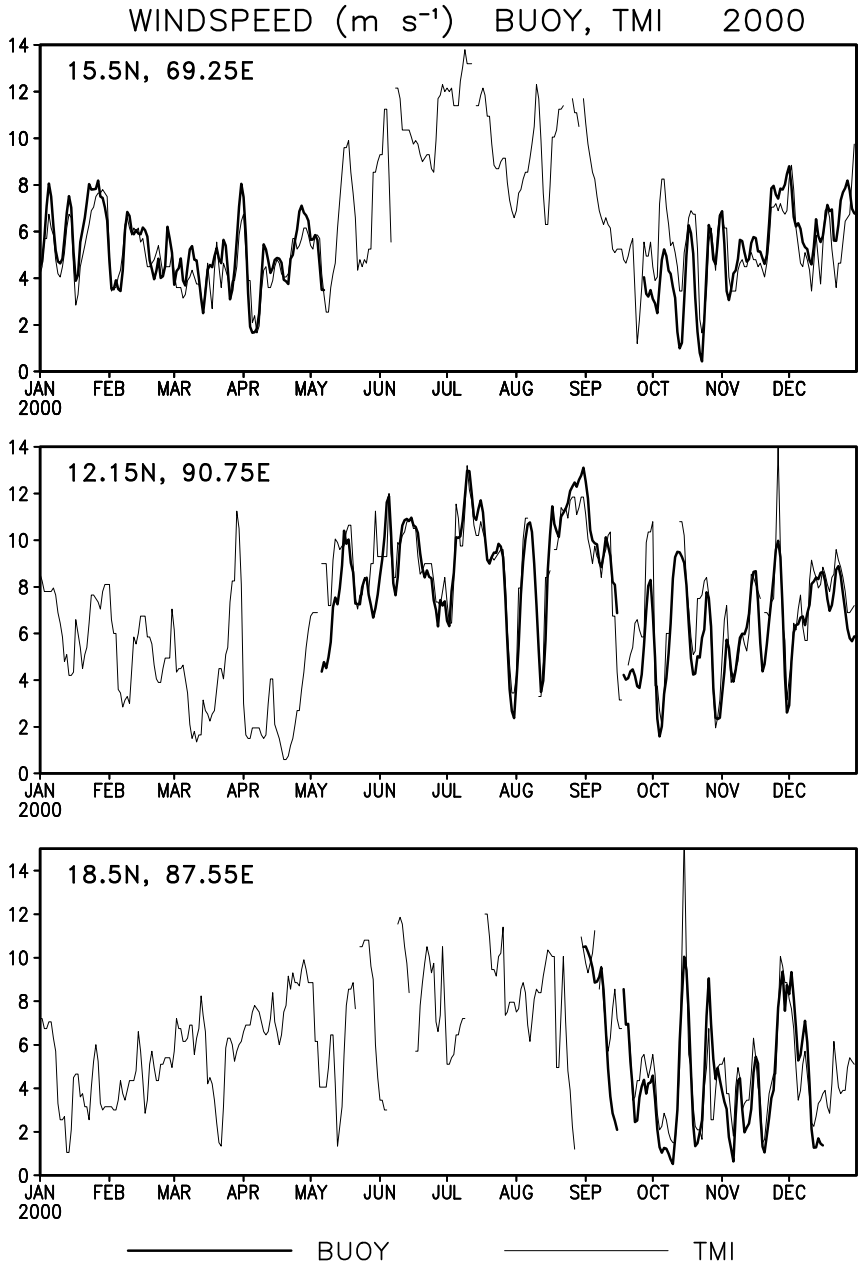

Figure 14: Wind speed (ms^{-1}) in 2000 from buoy (bold line) and TMI (thin line) at 15.5°N, 69.25°E (top), 12.15°N, 90.75°E (middle) and 18.5°N, 87.55°E (bottom).

7.2 Windspeed

There are considerable year-to-year differences in wind speed over the north Indian ocean. Windspeed over the entire Bay of Bengal was weaker in 1998 compared to 1999 or 2000 (Figures 17 and 18). Windspeed was also weaker over the south China Sea, the east equatorial Indian Ocean off Sumatra, and the tropical northwestern Pacific. Over the Bay of Bengal,

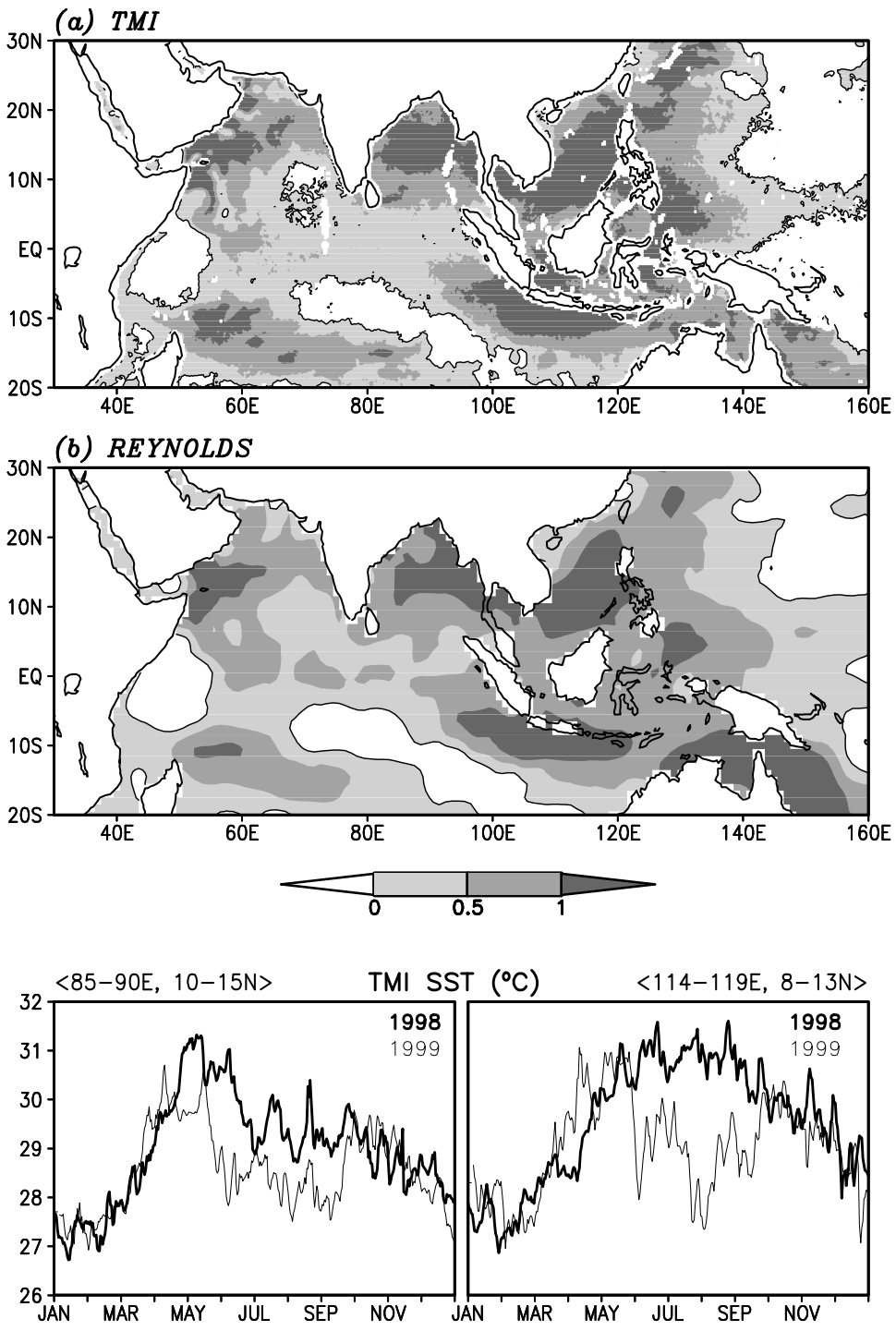

Figure 15: Difference in SST (°C) between 1998 and 1999 from (a) TMI and (b) Reynolds. Lower panel shows the time series of TMI SST averaged over 85-90°E, 10-15°N (left) and 114-119°E, 8-13°N (right) in 1998 (bold line) and 1999 (thin line).

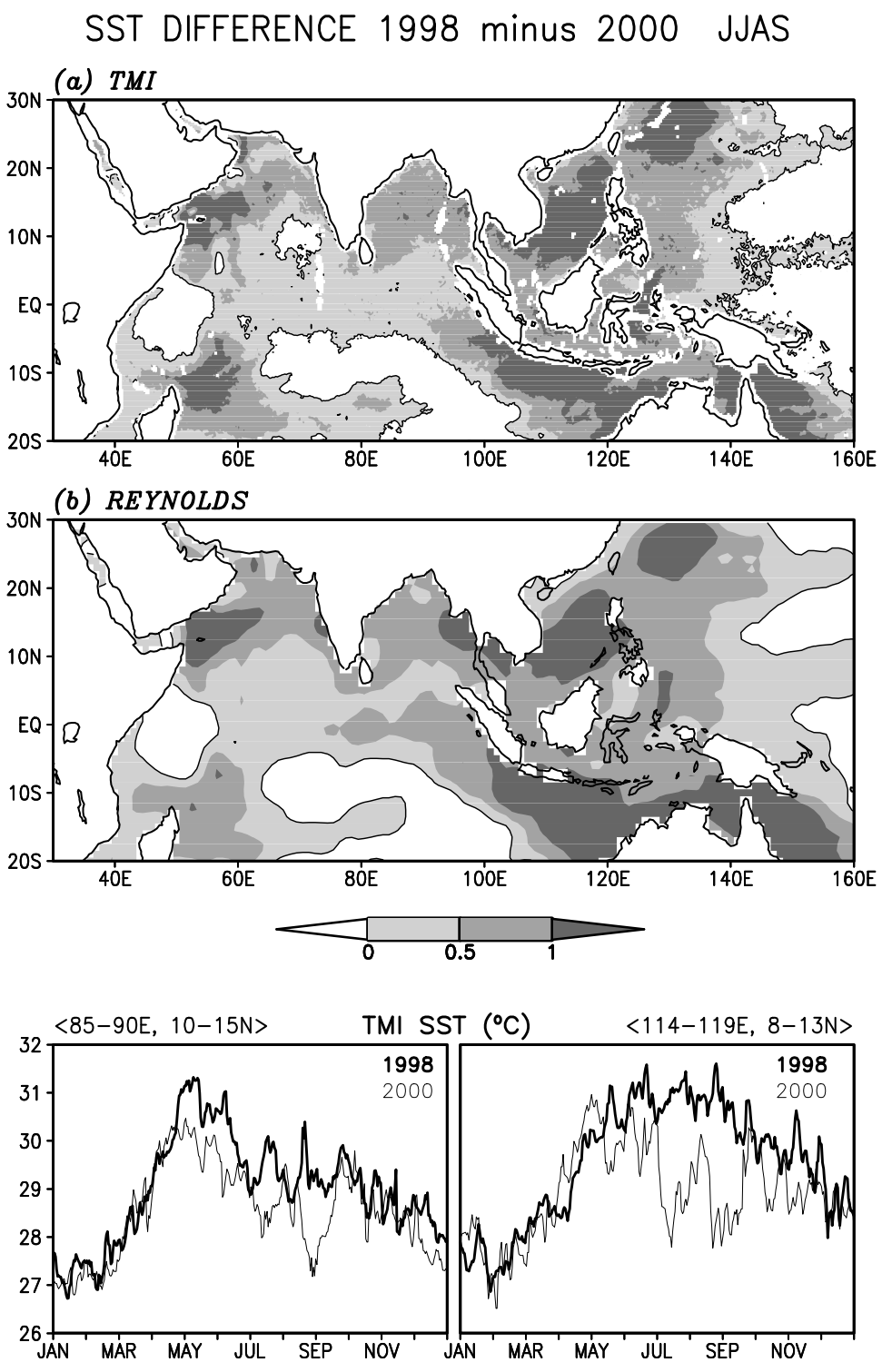

Figure 16: Difference in SST (°C) between 1998 and 2000 from (a) TMI and (b) Reynolds. Lower panel shows the time series of TMI SST averaged over 85-90°E, 10-15°N (left) and 114-119°E, 8-13°N (right) in 1998 (bold line) and 2000 (thin line).

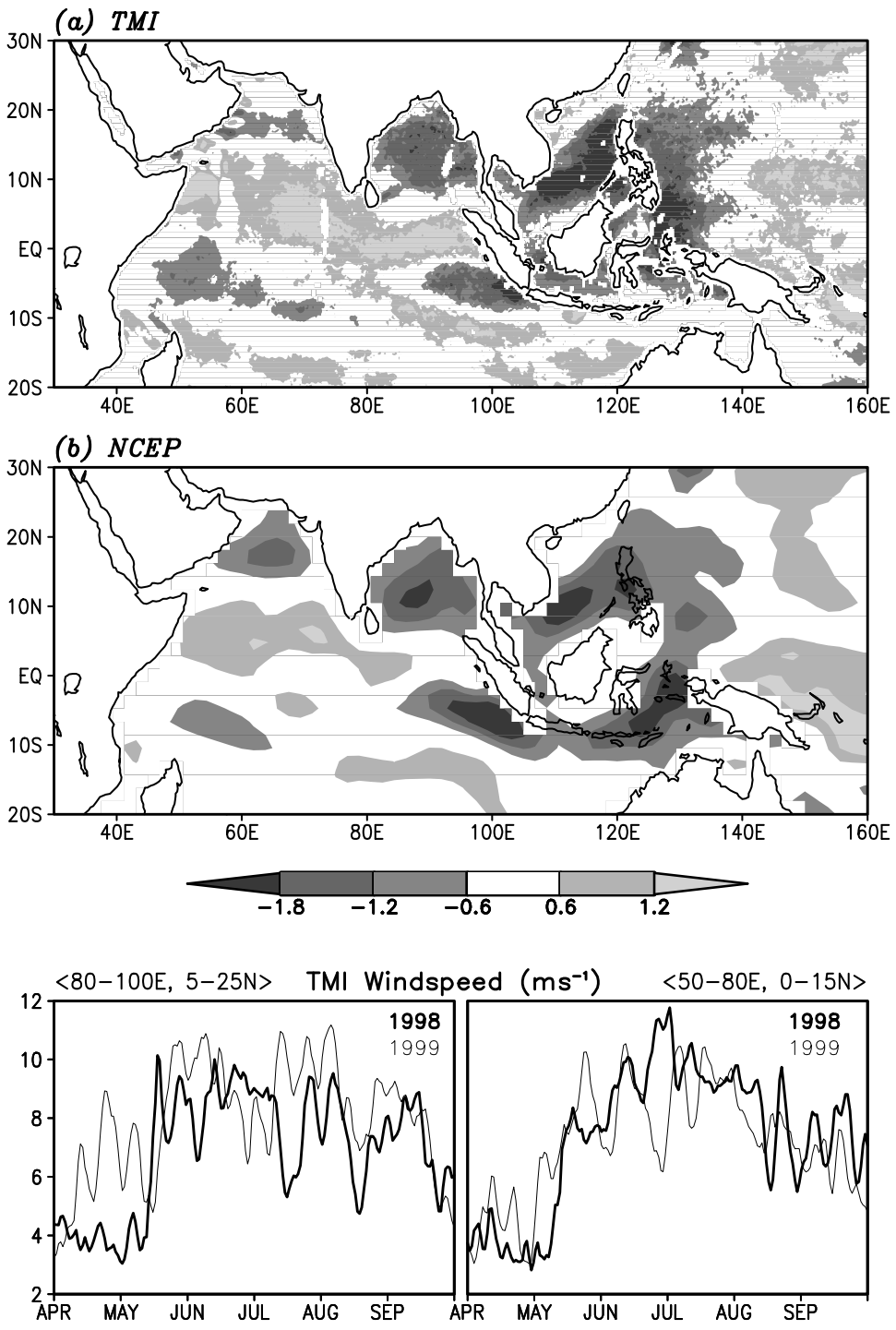

Figure 17: Difference in wind speed (ms^{-1}) between 1998 and 1999 from (a) TMI and (b) NCEP. Lower panel shows the time series of TMI wind speed averaged over 80-100°E, 5-25°N (left) and 50-80°E, 0-15°N (right).

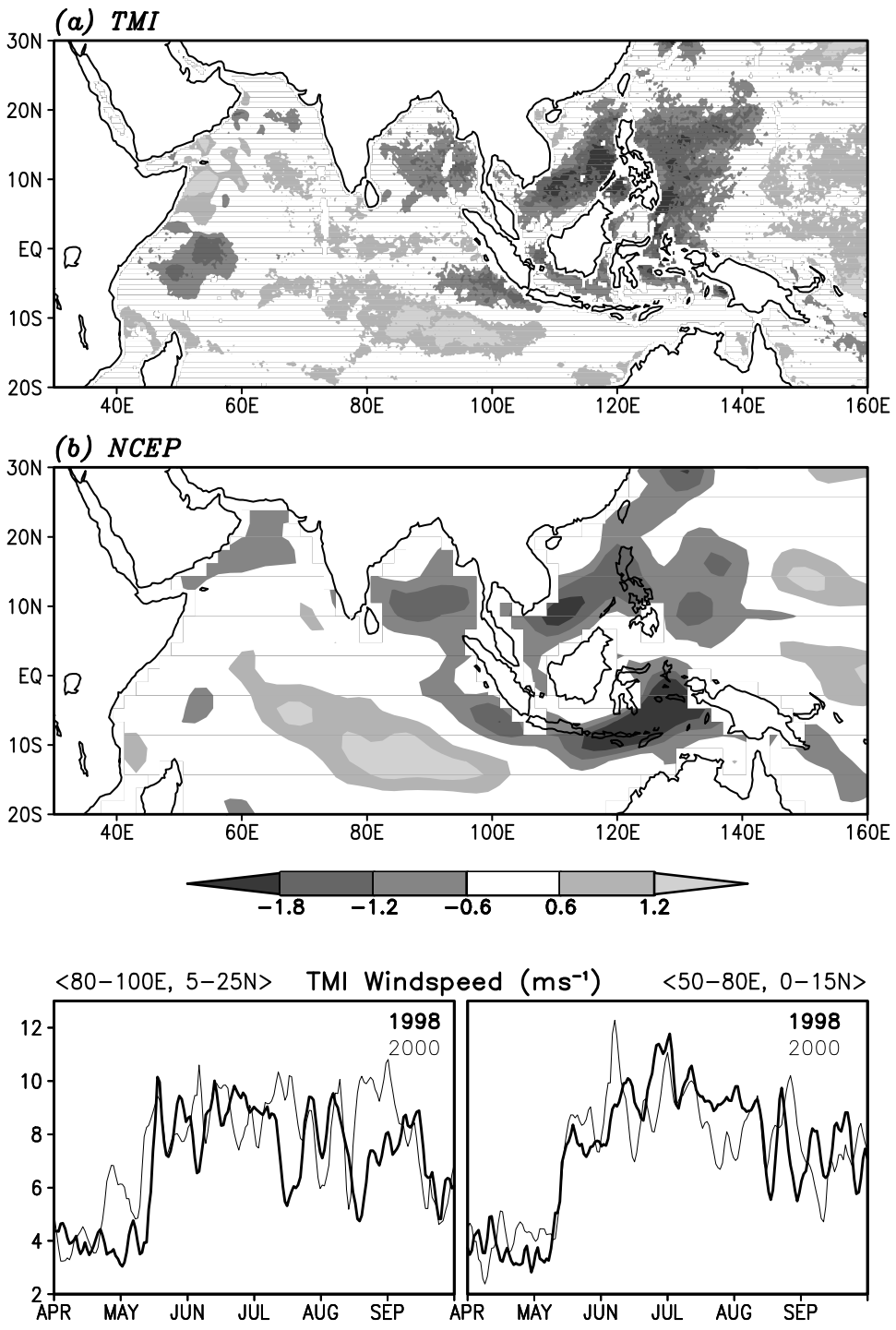

Figure 18: Difference in wind speed (ms^{-1}) between 1998 and 2000 from (a) TMI and (b) NCEP. Lower panel shows the time series of TMI wind speed averaged over 80-100°E, 5-25°N (left) and 50-80°E, 0-15°N (right).

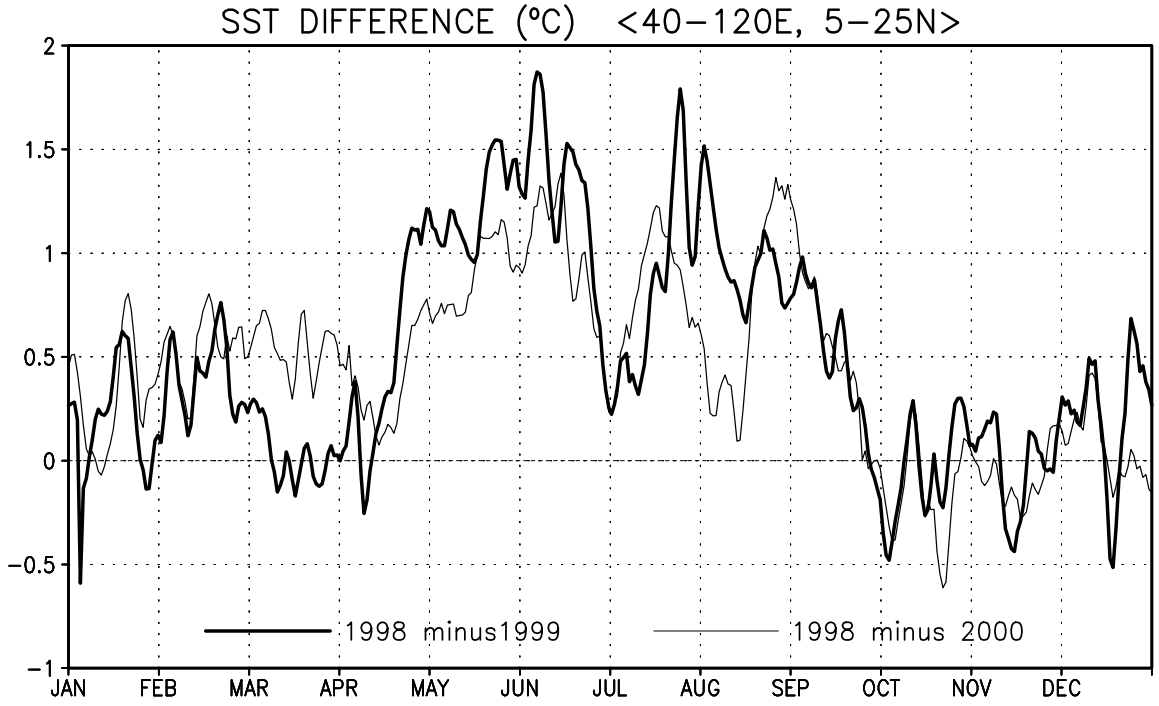

Figure 19: Difference in TMI SST (ms^{-1}) between 1998 and 1999 (bold line) and 1998 and 2000 (thin line) averaged over the north Indian Ocean: 40-120°E, 5-25°N.

the winds in 1998 were particularly weak during the pre-monsoon (Figure 17, bottom left panel). On the other hand, over the southern Arabian Sea, the winds were stronger in 1998 compared to 1999, but comparable to those in 2000 (Figure 18, bottom right panel). The areas of warmest anomalous SST in 1998 (Figures 15 and 16) are also the areas of lowest wind speed anomaly (Figures 17 and 18). Since the wind speed in 1998 was not lower than 1999 or 2000 throughout the north Indian Ocean, the basin wide average wind speed does not show anomalies lasting a season (Figure 20), unlike the basin wide SST differences shown in Figure 19.

8 Conclusion

Sea Surface Temperature and wind speed from the TRMM Microwave Imager is validated using observations from moored buoys in the north Indian Ocean. The most encouraging result is that, for the first time a product has become available that not only captures the intraseasonal and lower frequency variability on time scales longer than a few days, but

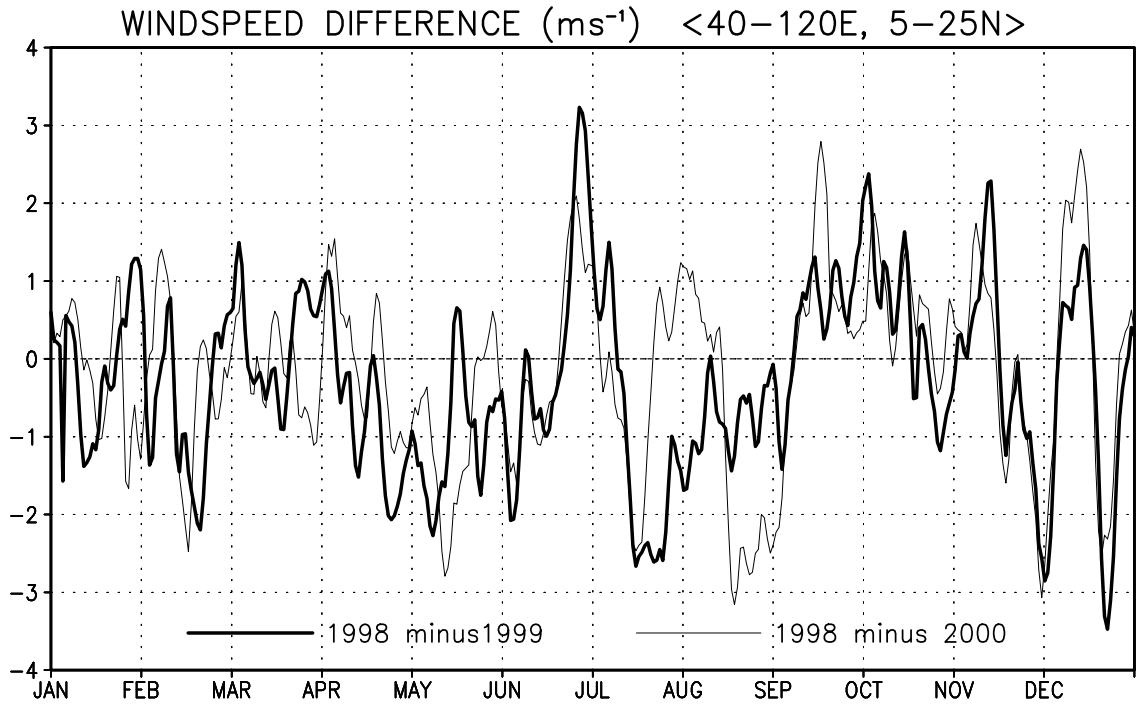

Figure 20: Difference in TMI SST (ms^{-1}) between 1998 and 1999 (bold line) and 1998 and 2000 (thin line) averaged over the north Indian Ocean: 40-120°E, 5-25°N.

also signatures of synoptic scale disturbances like tropical cyclones. Thus the TMI SST in conjunction with the wind speed, can be a useful tool for studies of basin-wide air-sea interaction on synoptic to interannual timescales.

Acknowledgements

We thank Frank Wentz of Remote Sensing Systems, CA, USA for making the TMI data available on their site ftp://ftp.ssmi.com. We also thank the Director, National Data Buoy Programme, NIOT, Chennai under the Department of Ocean Development, for providing the buoy data. We are grateful to M. Ravichandran of INCOIS, Hyderabad for many useful discussions regarding the buoy data. COADS and Levitus data are from the Climate Data Library at http://ingrid.ldgo.columbia.edu/. This work was partially funded by the Department of Science and Technology, New Delhi.

References

[1] Chelton, D. B., F. J. Wentz, C. L. Gentemann, R. A. de Szoeke and M. G. Schlax (2000): Satellite microwave SST observations of transequatorial tropical instability waves. *Geophys. Res. Lett.*, **27**, 9, 1239-1242.

[2] Grassl, H. (1976): The dependance of the measured cool skin of the ocean on wind stress and total heat flux. *Bound. Layer Meteorol.*, **10**, 465-474.

[3] da Silva, A. M., C. C. Young and S. Levitus (1994): *Atlas of surface marine data. Volumes 1 and 2*. U. S. Department of Commerce, NOAA, NESDIS.

[4] Kalnay, E., M. Kanamitsu, R. Kistler, W. Collins, D. Deaven, L. Gandin, M. Iredell, S. Saha, G. White, J. Woollen, Y. Zhu, A. Leetmaa, B. Reynolds, M. Chelliah, W. Ebisuzaki, W. Higgins, J. Janowiak, K. C. Mo, C. Ropelewski, J. Wang, R. Jenne, and D. Joseph (1996): The NCEP / NCAR 40-year Reanalysis Project. *Bull. Amer. Meteor. Soc.*, **77**, 437-471.

[5] Levitus, S. and T. P. Boyer (1994): *World Ocean Atlas 1994 Volume 4 : Temperature*, NOAA Atlas NESDIS **4**, U.S. Department of Commerce, Washington, D.C., 11pp.

[6] Rao, Y. R. and K. Premkumar (1998): A preliminary analysis of meteorological and oceanographic observations during the passage of a tropical cyclone in Bay of Bengal. NIOT technical note, NIOT-NDBP-TR 001/98.

[7] Reynolds, R. W. and T. M. Smith (1994): Improved global sea surface temperature analyses using optimum interpolation. *J. Clim.*, **7**, 929-948.

[8] Schlussel, P., W. J. Emery, H. Grassl and T. Mammen (1990): On the bulk-skin temperature difference and its impact on satellite remote sensing of Sea Surface Temperature. *J. Geophys. Res.*, **95**, 13,341-13,356.

[9] Sengupta, D., P. Joseph, R. Senan and G. Suresh Kumar (1999): Validation of NCEP daily surface winds over the north Indian ocean. *CAOS Report 99AS1*, Centre for Atmospheric and Oceanic Sciences, Indian Institute of Science, Bangalore.

[10] Wentz, F. J., C. Gentemann, D. Smith and D. Chelton (2000): Satellite measurements of Sea Surface Temperature through clouds. *Science*, **288**, 847-850.

[11] Wick, G. A., W. J. Emery, L. H. Kantha and P. Schlussel (1996): The behavior of the bulk - skin Sea Surface Temperature difference under varying wind speed and heat flux. *J. Phys. Oceanogr.*, **26**, 10, 1969-1988.